Cancer Immunology, Immunotherapy (2025) 74:238
https://doi.org/10.1007/s00262-025-04088-y

RESEARCH

NLRP3 activation promotes cGAS/STING signaling and antitumor immunity by colorectal cancer cells

Courtney Mowat[1] · Daniel Schiller[2] · Kristi Baker[1,3]

Received: 9 March 2025 / Accepted: 12 May 2025

Abstract

Introduction Colorectal cancer (CRC) is a highly prevalent and deadly disease that is largely refractory to immunotherapy. The only CRC subset that responds to these therapies is characterized by prevalent microsatellite instability (MSI), extensive CD8+ T cell infiltration and high expression of innate immune signaling pathways. Endogenous activation of the cGAS/STING pathway is essential for this CD8+ T cell antitumor response in MSI CRCs, suggesting that activating it in other CRCs could boost immunotherapy response rates. In contrast, activation of the NLRP3 inflammasome is typically associated with tumor-promoting inflammation although this has primarily been studied in immune cells.

Methods We used a mixture of flow cytometry, activation assays, in vivo orthotopic models and patient-derived organoids to investigate the effect of NLRP3 activation in CRC cells on cGAS/STING-mediated antitumor immunity.

Results Our results show that activation of the NLRP3 inflammasome specifically in CRC cells boosts cGAS/STING signaling in both MSI and non-MSI CRCs and that dual stimulation increases CD8+ T cell-mediated antitumor immunity. The ability of NLRP3 to enhance cGAS/STING signaling was specific and did not occur with activation of other innate immune pathways such as AIM2 or TLRs. Enhancement of cGAS/STING signaling by NLRP3 proceeded via a positive feedback loop that was inflammasome-independent and required early crosstalk between the signaling mediators and regulation of their gene expression.

Conclusions Activation of NLRP3 specifically in CRC cells could be a promising strategy to boost antitumor immunity in otherwise immunotherapy resistant CRCs.

Keywords Colorectal cancer · Microsatellite instability (MSI) · Antitumor immunity · cGAS/STING · NLRP3 inflammasome

Introduction

Colorectal cancer (CRC) is a highly prevalent disease arising in the generally immune-suppressive environment of the intestine [1, 2]. The majority of CRCs are thus immunologically cold and contain few infiltrating immune cells [3]. These CRCs are typically induced by *APC* mutations, and develop chromosomal instability (CIN) but have relatively few mutations [4]. In contrast, 15% of CRCs are immunologically hot and contain abundant CD8+ tumor infiltrating lymphocytes (TILs). These cancers are induced by loss of DNA mismatch repair due to hypermethylation of the *MLH1* promoter and develop widespread point mutations and microsatellite instability (MSI) [3]. These CRCs have a much more favorable prognosis due in part to the many neoantigens produced from their hypermutable genomes. However, it is now recognized that additional costimulatory pathways are strictly necessary to recruit and fully activate CD8+ TILs in CRC [5–7].

The type I interferon (IFN) pathway that produces IFNA/B is critical in this process and leads to production of key cytokines and chemokines essential for maximal CD8+ T cell activation and infiltration into the tumors [6, 7]. Type I IFN is strongly induced by the cGAS/STING cytosolic dsDNA-sensing pathway that evolved in all cells to

✉ Kristi Baker
kbaker2@ualberta.ca

[1] Department of Oncology, University of Alberta, Edmonton, Canada

[2] Department of Surgery, Royal Alexandra Hospital, Edmonton, Canada

[3] Department of Medical Microbiology and Immunology, University of Alberta, Edmonton, Canada

Published online: 07 June 2025

detect viral infection [8]. In MSI CRCs, this pathway is constitutively active due to endogenous generation of damaged DNA that leaks into the cytosol. This activates type I IFN signaling within the CRC cells and directly promotes recruitment and activation of the abundant TILs in MSI CRC [7]. Exogenous activation of this pathway in CIN CRCs can significantly enhance immune infiltration and improve response to immune checkpoint inhibitor (ICI) immunotherapies [9].

cGAS/STING are part of a family of pattern recognition receptors (PRRs) that regulate immune responses following activation by conserved molecular patterns such as specific nucleic acid configurations or microbial cell wall components [10]. Extensive crosstalk exists between these pathways, each of which is rarely activated in isolation, rendering it essential to understand how costimulation of other PRRs can alter cGAS/STING signaling and thus impact its potential as an immunotherapy target. An important PRR in the tumor microenvironment (TME) is the NLRP3 inflammasome which responds to various stress-associated molecules to trigger inflammation. Activation of NLRP3 is a two-step process first requiring transcriptional upregulation of NLRP3 itself and its target molecules, pro-IL1B and procaspase-1, followed by stimulation of the NLRP3 inflammasome assembly leading to cleavage and activation of IL1B and caspase-1 [11]. Crosstalk has previously been reported between the cGAS/STING and NLRP3 pathways in which cGAS/STING activation delivers the first signal required for transcriptional induction [12, 13]. The consequences of NLRP3 activation for antitumor immunity remain unclear [14–16]. While NLRP3-induced inflammation has indeed been associated with tumor progression, immunosuppression, and immunotherapy failure, it can also promote T cell activation and protect against CRC [17, 18]. Much of this discrepancy may result from the cell type being studied since most tumor-promoting effects have been found for NLRP3 activation in myeloid cells while most tumor promoting effects have been found for NLRP3 activation in T cells. The consequences for antitumor immunity of NLRP3 activation in CRC cells themselves have not been well studied despite the key immunomodulatory functions played by both intestinal epithelial cells and CRC cells [19].

Given the critical role for cGAS/STING signaling in promoting anti-CRC immune responses, we sought to clarify the role of NLRP3 activation in CRC cells on antitumor immunity. Our results show that NLRP3 activation promotes cGAS/STING signaling in both MSI and CIN CRC cells and significantly enhances activation of CD8+ T cell antitumor immunity in CRC. This is notably independent of caspase-1 activation, suggesting that the tumor promoting and tumor protective effects of NLRP3 may proceed via different downstream signaling pathways. These findings shed important light on the interplay between two dominant pathways in CRC antitumor immunity and suggest that selectively targeting both pathways in CRC cells could enhance immune eradication of all CRCs.

Materials and methods

Cell lines

MC38 murine CRC cells were purchased from Kerafast and maintained in high glucose DMEM supplemented with 10% FBS, 1% penicillin–streptomycin, and 1% HEPES at 37 °C with 5% CO_2. MSI and CIN variants of the cells were generated using CRISPR-Cas9 editing to delete *Mlh1* or mutate *Kras*, respectively, as described previously [6, 20]. *Sting* knockdown in the MSI MC38 CRC cells was generated as described previously using shRNA and the pLKO.1 system [6, 21]. Ovalbumin (OVA) expressing MSI and CIN MC38 CRC cells were made by transfection with the pCI-neo-cOVA plasmid (Addgene #25097) and selection with 200 µg/ml G418 [22].

Cell treatments

MC38 CRC cells were seeded into plates 24 h before treatments as indicated in the figure legends. The following agonist treatments were used: 9 µg/ml 2',3'-cGAMP, 2 mM ATP (Millipore Sigma), 10 µM BMS-986299 (MedChemExpress), or 0.1 µg/ml IL18 (BioLegend). cGAMP was delivered to the cells encapsulated in Lipofectamine 2000 (Thermo Fisher). In some cases, cells were first pretreated for 1 h with the following inhibitors (2 µM H-151, 10 µM MCC950 (InvivoGen)) before addition of the agonist treatments. For siRNA-mediated knockdown, cells were treated with 2 nM siRNA against *Nlrp3* or a scrambled control (TriFECTa Kit DsiRNA Duplex (Integrated DNA Technologies)) delivered with Lipofectamine RNAiMAX (Thermo Fisher) for 24 h before addition of agonists. After the indicated treatment times, cell supernatant or cells were harvested.

Immunofluorescence staining

Cells were seeded onto coverslips coated with CellTak (Corning) and allowed to adhere overnight at 37 °C. Cells were fixed with methanol and blocked (5% normal serum, 0.3% Triton X-100 in PBS). Cells were stained with the indicated primary antibodies for 1 h at room temperature. After washing, cells were stained with secondary antibodies (Thermo Fisher) for 1 h at room temperature followed by phalloidin Alexa^{546} (Thermo Fisher) for 20 min. Nuclei were stained with DAPI and then coverslips were mounted on slides. Cells were imaged on a Leica Falcon SP8 STED

System. Post image processing was performed using ImageJ [23]. See Table S1 for all antibodies.

Western blotting

Protein was isolated in lysis buffer (50 mM Tris–HCl, 150 mM NaCl, 50 mM sodium pyrophosphate, 1 mM EDTA, 0.5% NP40, 1% Triton X-100) containing 1 mM sodium orthovanadate, and 1 × protease inhibitor (Millipore Sigma). Protein was quantified using a BCA assay (Thermo Fisher) and 5 or 10 µg of protein was loaded on SDS-PAGE gels and transferred to nitrocellulose membranes. See Table S1 for all antibodies. Bands were visualized using the ECL Prime Western Blotting Detection Reagent (Cytiva). Pixel density was quantified using ImageJ and normalized to the respective loading controls [23].

RNA and qPCR

RNA was extracted using Trizol (Invitrogen) and reverse transcribed using the High-Capacity cDNA Reverse Transcription Kit (Thermo Fisher). qPCR was performed with the primers in Table S2 using the POWRUP SYBR Master Mix (Thermo Fisher). qPCR was performed on the QuantStudio6 real-time PCR system (Applied Biosystems).

Mouse CRC experiments

C57BL/6 wildtype mice originally purchased from Charles River were bred and maintained in the Cross Cancer Institute vivarium. OT-I mice were purchased from The Jackson Laboratory. Mixed groups of male and female littermates between the age of 6–20 weeks old were used for experiments. All animal work was approved by the Cross Cancer Institute's Animal Care Committee.

Subcutaneous CRC experiments were performed by injecting 5×10^5 MSI or CIN MC38 CRC cells in 100 µl PBS into the hind flank. Tumors were harvested after 2–3 weeks. Tumors were dissociated in an enzyme cocktail of RPMI containing 0.5 mg/ml collagenase IV (Millipore Sigma), 10 µg/ml DNaseI (Millipore Sigma), 10% FBS, 1% penicillin–streptomycin and 1% HEPES buffer for 30 min at 37 °C in a shaking incubator at 200 rpm [6, 24]. Fragments were rigorously pipetted to dissociate, filtered through a 100 µm cell strainer and washed. Cancer and immune cells in the tumors were separated using a 40/80% percoll gradient (Cytiva), at 500 g for 30 min at room temperature. The top layer (tumor cells) and the interface (immune cells) were collected separately, washed, and processed for RNA isolation as above.

Orthotopic CRC experiments were performed by injecting 1.5×10^5 MC38 CRC cells in 50 µl PBS into the wall of the descending colon using a flexible needle (Hamilton) inserted through the working channel of a Wolfe endoscope and visualized via the ColoView imaging system (Storz) [6, 25]. In some experiments, mice were treated intraperitoneally every 3 days with either 1 mg/kg ADU-S100 and 200 µg anti-PD1/isotype (BioXcell) or with 20 mg/kg MCC950. Orthotopic tumors, MLNs and spleen were harvested after 14–21 days and dissociated as above before flow staining.

Mouse and human CRC-derived organoids

Murine organoids were generated from colorectal tumors induced in wildtype C57BL/6 mice by repeated doses of azoxymethane (Millipore Sigma) (10 weekly doses of 10 mg/kg azoxymethane) as previously described and cultured as below [6, 26].

Human CRC organoids were generated as described previously from resected tumors [6, 26]. Briefly, tumors were dissociated for 1 h in DMEM with 2.5% FBS, 75 U/ml collagenase XI (Millipore Sigma), 125 µg/ml dispase II (Millipore Sigma). Following filtration, cells were plated at 500–1000 per well in growth factor reduced Matrigel (Corning) and cultured in basal crypt media (Advanced DMEM/F12containing 10% FBS, 2 mM glutamine, 10 mM HEPES, 1 mM N-acetylcystein, 1X N2 supplement, 1X B27 supplement, 10 mM nicotinamide, 500 nM A83-01, 10 µM SB202190, 50 ng/ml EGF) (Thermo Fisher) mixed 1:1 with conditioned supernatant from L-cells expressing Wnt3a, R-spondin and noggin (ATCC #CRL-3276) [27]. All work with human samples was approved by the Health Research Ethics Board of Alberta Cancer Committee and carried out after obtaining informed patient consent.

Primary MSI variants of the mouse and human organoids were generated using lentiviral transduction with the pLKO.1 system and shRNA sequences in Table S2 [6, 21, 25]. Briefly, organoids were pretreated for 4–5 days with 10 mM nicotinamide before being dislodged from the plate by pipetting and treated for 5 min at 37 °C with TrypLE Express (Life Technologies). Organoids were mixed with concentrated lentivirus along with 8 µg/ml polybrene and 10 µM Y27632 (Millipore Sigma) and seeded into a 96-well plate. The plate was centrifuged for 60 min at 600 g at 32 °C and then incubated at 37 °C for 6 h. The organoids were then embedded in Matrigel and cultured in media containing 50–100 µg/ml hygromycin to select for successful transduction. Gene knockdown was verified by Western blot.

For stimulations, equal numbers of organoids were plated in Matrigel and cultured for 3 days before being treated as indicated in the figure legends. Organoids were harvested by resuspending in ice cold Cell Recovery Solution (CRS) (Corning) to dissolve the Matrigel, diluted in ice cold PBS, spun down and processed for RNA or protein isolation.

Flow cytometry, ROS and cytokine bead arrays

Flow cytometry staining was performed using the antibodies in Table S1 and the Zombie Aqua viability stain (BioLegend). Briefly, cells were washed and stained with a cocktail of the relevant antibodies and Zombie Aqua, each at a 1/300 dilution, for 30 min at 4 °C. Cells were washed before fixing and permeabilizing using the Foxp3 Transcription Factor Staining Buffer Set (eBioscience) according to the manufacturer's directions. Samples were then stained with antibodies against intracellular targets, each at a 1/300 dilution, for 30 min at 4 °C. Samples were then washed and analyzed on a CytoFlex S cytometer (Beckman Coulter) with subsequent analysis using FlowJo v9 (BD Biosciences).

ROS generation was quantified using an H2DCFDA kit (ThermoFisher) following the manufacturer's directions and analyzed on a Cytoflex S cytometer.

Secretion of CCL5 and CXCL10 by MSI and CIN CRCs into cell supernatants was analyzed using a custom LegendPlex cytokine bead array (BioLegend, catalog #900001178). Briefly, 5×10^5 cells per well were seeded in 200 µl into 96-well plates and grown for 24 h. The supernatant was the collected and cleared by centrifugation (500 g for 5 min at 4 °C) and frozen at − 80 °C until use. Cytokine content of the supernatant was analyzed using the LegendPlex kit according the manufacturer's instructions. Cytokines included in the assay panel were: CCL2 (MCP-1), CCL5 (RANTES), CXCL1 (KC), CXCL10 (IP-10), IFN-α, IFN-β, IFN-γ, IL-10, IL-12p70, IL-18, IL-1β, IL-6, TNF-α. Data was acquired on a CytoFlex S cytometer and analyzed in FlowJo v9.

T cell activation assays

CD8+ T cells were isolated from the spleens and lymph nodes of OT-I mice using the EasySep Mouse CD8+ T Cell Isolation Kit (StemCell Technologies). For direct co-culture experiments, OVA-expressing MSI and CIN CRC cells were first treated for 24 h followed by extensive washing. CD8+ T cells were then added at a 5:1 T cell:tumor cell ratio and cultured for 24–48 h. Cytotoxicity was assessed using the CellEvent Caspase-3/7 Green Detection Reagent (Thermo Fisher) at 1.0 µM and gating on CD45-negative cells. To assess T cell activation by STING knockdown or scramble controls, CRC cells were treated for 24 h and then pulsed with 1 µg/ml of the SIINFEKL peptide for 30 min before being washed and cultured with OT-I CD8+ T cells as above.

Data from The Cancer Genome Atlas analysis

Human RNA sequencing data and DNA sequencing data (Illumina HiSeq RNASeqV2) from the Colorectal Adenocarcinoma dataset from the TCGA Nature 2012 and TCGA PanCancer Atlas from The Cancer Genome Atlas were downloaded from cBioPortal for Cancer Genomics (https://www.cbioportal.org/) [28–30]. Data was log2 transformed and analyzed using the DESeq2 package in R (v3.0) [31].

Statistical analysis

Prism (GraphPad Software Inc.) was used for statistical analysis. Comparisons of two unpaired groups was made by two-tailed Student's t-test for normal data, or Mann–Whitney for non-parametric tests. For three or more groups with two parameters, two-way ANOVA or multiple t-test procedures were used as appropriate for data with Gaussian distribution. Analysis of responses to multiple stimuli of a single cell type or of cells from a single donor were analyzed using paired tests. Post-hoc analysis to correct for multiple comparisons and detect differences between groups was by the two-stage linear step-up procedure of Benjamin, Krieger and Yekutieli with false discovery rate < 0.05. A two-sided probability (P) of alpha error less than 0.05 defined significance.

Results

NLRP3 stimulation enhances cGAS/STING signaling in CRC cells

To investigate the effects of NLRP3 activation on cGAS/STING signaling in CRC cells with different baseline levels of cGAS/STING activation, we generated MSI and CIN variants of the mouse MC38 CRC cell line by deleting *Mlh1* or mutating the CIN-associated gene *Kras*, respectively [6]. We then stimulated these with either the cGAS agonist 2′3'-cGAMP (cGAMP), the NLRP3 agonist ATP, or both, and examined activation of downstream signaling mediators. As shown in Fig. 1, dual stimulation clearly upregulated mediators of both signaling pathways more than either pathway-specific ligand alone. In particular, addition of ATP to cGAMP induced stronger activation of STING itself as well as of TBK1 and NFKB (Fig. 1A). To confirm the specificity of these results and truly demonstrate the role of NLRP3 in boosting cGAS/STING activation, we used a second NLRP3 agonist, BMS-986299, in place of ATP and demonstrated that this also increased activation of TBK1 in the presence of cGAMP (Figs. 1B, S1A). Furthermore, this activation was inhibited by knocking down NLRP3 with a specific siRNA but not a control siRNA. Addition of ATP to cGAMP also greatly upregulated expression of the chemokines CCL5 and CXCL10 (Fig. 1C) as well as the production of ROS (Fig. 1D) [6]. CCL5 and CXCL10 are prominent IFN-stimulated genes and are required

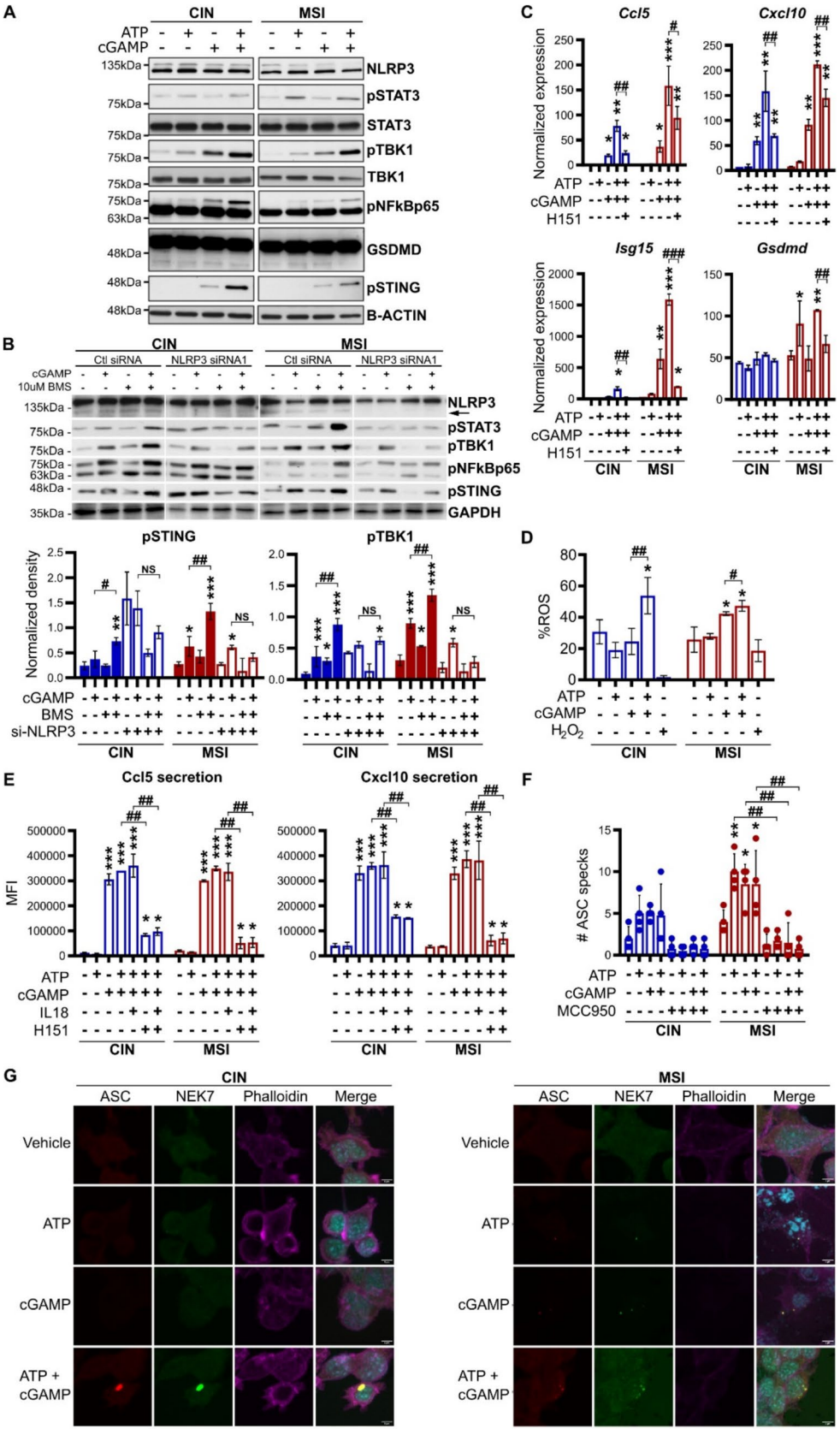

Fig. 1 NLRP3 enhances cGAS/STING signaling in MSI and CIN CRC cells. **A** MSI or CIN MC38 CRC cells were stimulated for 24 h with 9 µg/ml 2'-3'-cGAMP and/or 2 mM ATP. Activation of signaling pathway mediators was then assessed by Western blotting. **B** siRNA was used to knock down NLRP3. 24 h later, CRC cells were stimulated with 9 µg/ml 2'-3'-cGAMP and/or 10 µM BMS-986299 for a further 4 h before protein isolation and Western blotting. Pixel density was quantified using ImageJ and normalized to the respective loading controls. See Fig. S1A. **C–E** Cells were stimulated as in (**A**) and expression of downstream products was assessed by qPCR (**C**), ROS assay (**D**), or flow cytometric bead assay of cell supernatants (**E**). Where indicated, cells were first pretreated for 1 h with 2 µM H151, 10 µM MCC950 or 0.1 µg/ml IL18. (**F–G**) MSI and CIN CRC cells were stimulated as indicated for 4 h and then evaluated by confocal microscopy for colocalization of ASC and NEK7 in ASC specks. Quantification is shown in (**F**) and representative images in (**G**). Scale bar = 5 µm. All panels show representative data from $N \geq 3$ experiments each with ≥ 2 biological replicates. For all panels, the * symbols show significance of the indicated bar relative to the corresponding vehicle control: $^{*}p \leq 0.05$, $^{**}p \leq 0.01$, $^{***}p \leq 0.001$ (*t*-test). For all panels, the # symbols show significance between the two indicated samples: $^{\#}p \leq 0.05$, $^{\#\#}p \leq 0.01$, $^{\#\#\#}p \leq 0.001$ (ANOVA)

for CD8+ T cell recruitment into MSI CRCs. While addition of ATP to cGAMP did increase secretion of CCL5 and CXCL10 (Fig. 1E), the effect was considerably smaller in magnitude than for mRNA expression of these genes, which we suspect was either due to degradation of the cytokine or its consumption by the cells themselves over the 24 h culture period. In addition, we were unable to detect significant secretion of IFNβ by the CRC cells, which we suspect is due to the low levels of secretion of this inflammatory cytokine known to be produced by epithelial and cancer cells [6, 32]. Nonetheless, our data provide strong evidence that NLRP3 activation in CRC cells can enhance activation of cGAS/STING signaling.

To confirm that our stimulation conditions were appropriately activating the canonical NLRP3 pathway, we examined ASC-NEK7 speck formation. This showed that addition of ATP, cGAMP or both all led to similar increases in speck formation (Fig. 1F–G), confirming that ATP in our system activated the expected NLRP3 signaling pathway and that, as others have shown, cGAS/STING stimulation can directly activate NLRP3 [12, 13]. Dual activation of the pathways could be reversed by addition of the STING inhibitor H151 (Fig. 1C,E) or the NLRP3 inhibitor MCC950 (Fig. 1F) but was not enhanced by addition of the NLRP3 inflammasome product IL18 (Fig. 1E), indicating that interaction between these pathways relies on initial intracellular mechanisms and not on later downstream signaling induced by gene expression changes. Notably, in most cases, dual stimulation led to equal activation of the cGAS/STING and NLRP3 pathways in both MSI and CIN CRC cells. This confirms our recent finding that there are no fundamental defects in these signaling pathways within CIN CRC cells and that they are equally sensitive to external ligands despite having lower baseline levels due to minimal production of endogenous ligands compared to MSI CRC cells [6].

Despite the clear enhancing effect we observed for NLRP3 stimulation on cGAS/STING signaling, ATP stimulation alone did not activate cGAS/STING signaling (Fig. 1A–E). It thus appears that STING and NLRP3 activation work together to enhance STING activity via a positive feedback loop rather than STING simply increasing expression of NLRP3 mediators that then act independently. To directly test this, we knocked-down *Sting* in MSI MC38 CRC cells ($MSI^{StingKD}$). This abrogated not only enhancement of cGAS/STING signaling by NLRP3 (Figs. 2A–B, S1B) but also decreased expression of the NLRP3 products pro-*IL18* (Fig. 2B) and cleaved caspase-1 (Fig. 2A). This is consistent with a dual mechanism where cGAS/STING activation regulates NLRP3 signaling mediators that then establish a positive feedback loop to directly increase cGAS/STING pathway activation.

To determine the potential mechanism of NLRP3-mediated cGAS/STING enhancement, we tested whether it involved the canonical NLRP3 signaling pathway that activates caspase-1. However, addition of the caspase-1 inhibitor YVAD to the dual stimulation of CRC cells did not decrease cGAS/STING activation by NLRP3, indicating that the enhancement is caspase-1-independent (Fig. 2C) [13, 33]. Given that most effects of NLRP3 depend on caspase-1 activation, our data suggest a specific and possibly unique cooperativity between cGAS/STING and NLRP3. To further study this, we looked at some of the many other PRRs that could influence cGAS/STING signaling by testing whether activation of two additional PRR pathways could recreate the effect we observed with NLRP3. Stimulation of CRC cells with only poly(dA:dT), an agonist of several PRRs including the AIM2 inflammasome, directly increased expression of the STING pathway products *Ccl5*, *Cxcl10* and *Isg15* in addition to the inflammasome target pro-*Il18* (Fig. S2A) [34]. However, there was no cooperativity between AIM2 and cGAS/STING since addition of cGAMP did not increase activation beyond that of poly(dA:dT) alone. In contrast, stimulating our CRC cells with only flagellin, a TLR5 agonist, did not directly increase expression of *Ccl5*, *Cxcl10*, *Isg15* and pro-*Il18* at all or enhance the stimulatory potential of cGAMP (Fig. S2B) [35]. It thus appears that while some PRRs can promote cGAS/STING pathway signaling alone, cooperativity with cGAS/STING is not a general feature of all PRRs but rather specific to the NLRP3 inflammasome, making this a uniquely attractive target for therapeutic cGAS/STING modulation.

NLRP3 in CRC cells promotes activation of CD8+ T cell-mediated antitumor immunity by cGAS/STING signaling

NLRP3 inflammasome activation is typically associated with tumor-promoting inflammation while cGAS/STING stimulation typically induces activation of tumor-protective T cell activation. To determine if activating NLRP3 in CRC cells could specifically potentiate cGAS/STING-mediated activation of antitumor CD8+ T cells, we stably transduced $Mlh1^{-/-}$ and $Kras^{Mut}$ MC38 CRC cell lines with the model tumor neoantigen ovalbumin (OVA) to generate MSI^{OVA} and CIN^{OVA} cells, respectively. We then pre-treated these cells with ATP and/or cGAMP for 24 h, removed the treatment, and then cocultured the CRCs with OVA-specific OT-I CD8+ T cells. Dual stimulation of both MSI^{OVA} and CIN^{OVA} CRC cells with cGAMP and ATP significantly increased activation of CD8+ T cells compared to either vehicle or cGAMP treatment alone (Figs. 3A-B, S3). Surprisingly, CRC cells stimulated with the NLRP3 ligand ATP alone also activated significantly more CD8+ T cells than did either the vehicle or cGAMP (Fig. 3A). Thus, NLRP3 stimulation alone can induce a productive antitumor immune response in both MSI and CIN CRC cells, although the effect was strongest in MSI

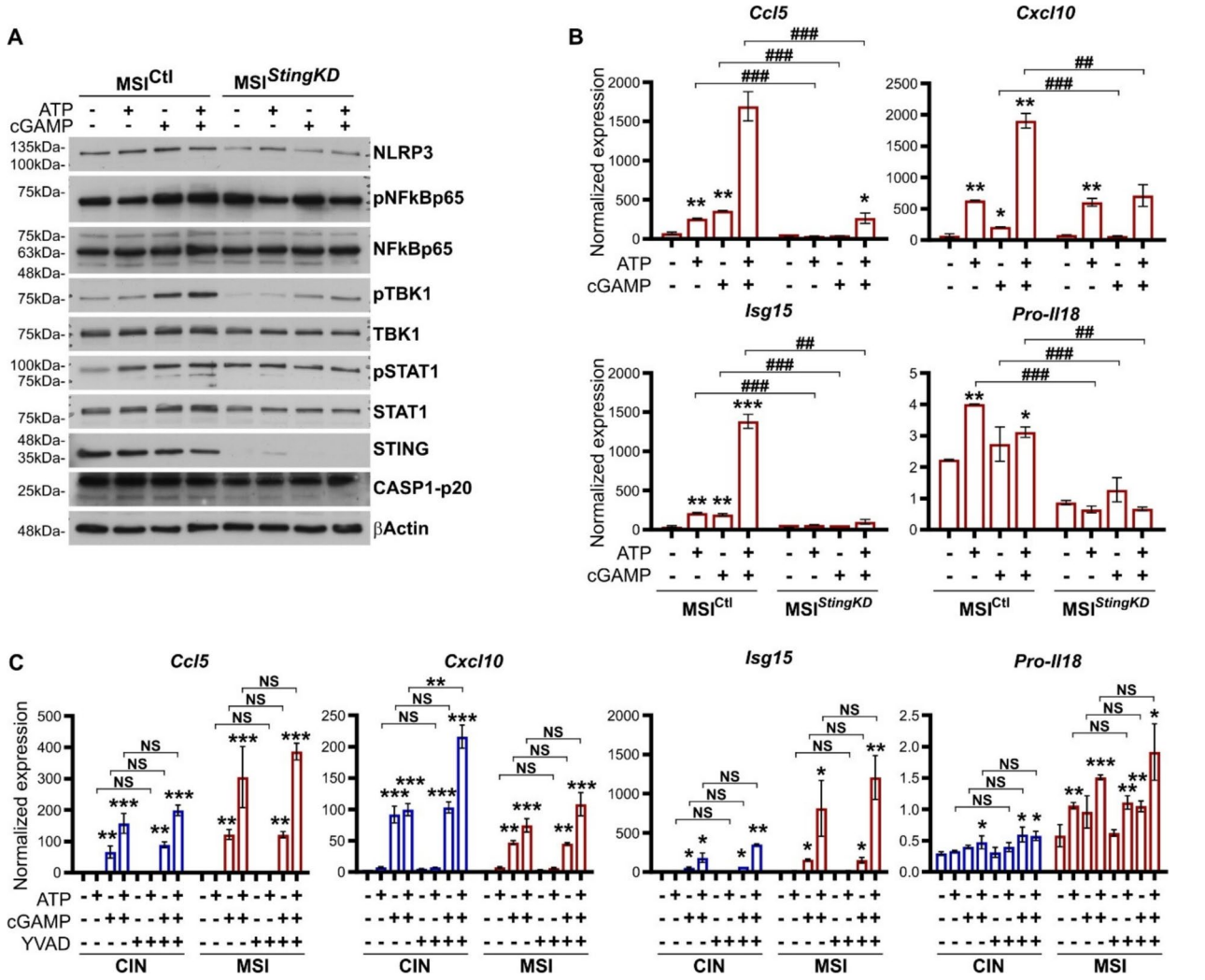

Fig. 2 NLRP3-mediated activation of cGAS/STING in CRC cells establishes a caspase-1-independent positive feedback loop. (**A, B**) *Sting* expression was stably knocked down in the MSI MC38 CRCs to generate MSI^{StingKD} cells. Cells were stimulated for 24 h with 9 µg/ml 2'-3'-cGAMP and/or 2 mM ATP and activation of signaling pathways was evaluated by Western blotting (**A**) while expression of downstream products was evaluated by qPCR (**B**). Pixel density for **A** was quantified using ImageJ and normalized to the respective loading controls. See Fig. S1B. **C** Cells were stimulated for 24 h with 9 µg/ml 2'-3'-cGAMP and/or 2 mM ATP and addition to 10 µg/ml YVAD (caspase-1 inhibitor). RNA was subsequently isolated and gene expression evaluated by qPCR. All panels show representative data from $N \geq 3$ experiments each with ≥ 2 biological replicates. For all panels, the * symbols show significance of the indicated bar relative to the corresponding vehicle control: $^{*}p \leq 0.05$, $^{**}p \leq 0.01$, $^{***}p \leq 0.001$ (t-test). For all panels, the # symbols show significance between the two indicated samples: $^{\#\#}p \leq 0.01$, $^{\#\#\#}p \leq 0.001$ (ANOVA)

CRCs. Similar results were observed when using the more NLRP3-specific agonist BMS-986299, supporting the NLRP3 dependence and specificity of the observed antitumor T cell enhancement effect (Fig. 3C). This was further bolstered by showing that enhancement was absent in the presence of an *Nlrp3*-depleting siRNA. To confirm these data and determine the extent to which this effect was dependent on the ability of NLRP3 to directly activate the cGAS/STING pathway in the CRC cells, we stimulated MSI^{StingKD} CRCs cells with ATP, cGAMP or both. NLRP3 activation failed to enhance CD8+ T cell activation in these STING-deficient cells despite activating CD8+ T cell activation by the control cells (Fig. 3B). Collectively, these data show that dual activation of both cGAS/STING and NLRP3 in MSI and CIN CRC cells cooperatively induces antitumor immunity and suggests that one way to maximize CD8+ T cell activation in CIN CRC patients would be to treat them with therapeutics that stimulate both pathways.

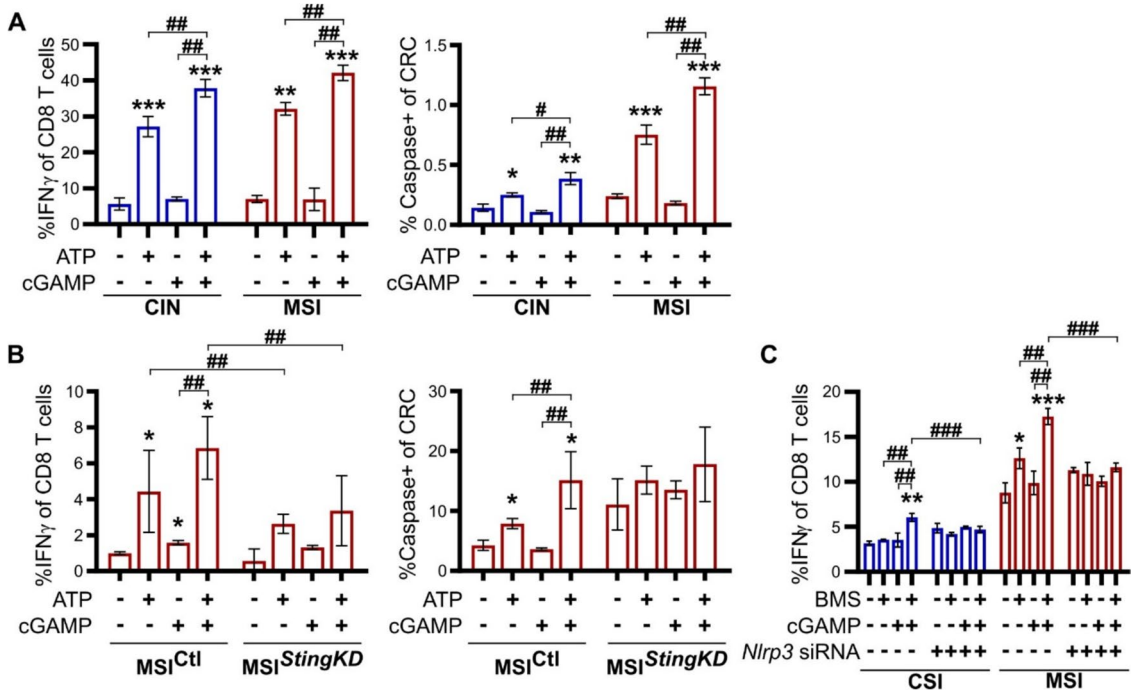

Fig. 3 Costimulation of NLRP3 and cGAS/STING in CRC cells promotes activation of CD8+ T cell-mediated antitumor immunity. **A** OVA-expressing MSI and CIN MC38 CRC cells were stimulated for 24 h with 9 µg/ml 2'-3'-cGAMP and/or 2 mM ATP. The cells were then washed and cocultured for an additional 48 h with OT-I CD8+ T cells. **B** *Sting* expression was stably knocked down in the MSI MC38 CRCs to generate $MSI^{StingKD}$ cells. 24 h later, cells were treated as in (**A**). **(A-B, left panels)** Activation of CD8+ T cells was measured by intracellular flow cytometry. **(A–B right panels)** T cell-mediated killing of the CRC cells was measured by caspase 3/7 cleavage. **C** siRNA was used to knock down NLRP3 in OVA-expressing MSI and CIN CRC cells. 24 h later, CRC cells were stimulated with 9 µg/ml 2'-3'-cGAMP and/or 10 µM BMS-986299 for a further 24 h before washing and coculture with OT-I CD8+ T cells. After an additional 48 h, T cell activation was examined. All panels show representative data from N = 3 experiments with 2–3 biological replicates per experiment. For all panels, the * symbols show significance of the indicated bar relative to the corresponding untreated control: $*p \le 0.05$, $**p \le 0.01$, $***p \le 0.001$ (t-test). For all panels, the # symbols show significance between the two indicated samples: $^{\#}p \le 0.05$, $^{\#\#}p \le 0.01$ (ANOVA)

NLRP3 activation in CRC cells promotes cGAS/STING-mediated antitumor immunity under physiological conditions

To determine the relevance of our observations to human CRC patients, we mined the PanCancer Atlas CRC dataset in The Cancer Genome Atlas (TCGA) database to examine the relationship between NLRP3 and cGAS/STING mediators [28–30]. We noted that MSI CRCs have significantly higher mRNA expression of both *STING* and *NLRP3* (Fig. 4A), as well as of many of the canonical products associated with both signaling pathways (Fig. 4B). These data suggest that both pathways might be activated under similar conditions, providing opportunities for cross-talk between them.

To more fully elucidate the dynamics between NLRP3 and cGAS/STING in a physiologically relevant setting, we used two in vivo models. MSI and CIN MC38 CRC variants were first injected subcutaneously into the flanks of immunocompetent C57BL/6 mice. We confirmed immunohistochemically and by flow cytometry that the $Mlh1^{-/-}$ MSI tumors contained greater numbers of CD8+ TILs and expressed higher levels of STING than the CIN tumors and thus phenocopied the main characteristics of MSI CRC in patients (Fig. 5A, B). When we examined NLRP3 and phospho-STING (pSTING) expression in the tumor cells, we noted that each was negatively correlated with tumor mass regardless of whether the tumors were MSI or CIN (Fig. 5C). This suggested a role for both of these signaling pathways in promoting antitumor immunity. Interestingly, we found a very strong correlation between the expression of pSTING and NLRP3 within the tumor cells themselves, confirming the known link between activation of these pathways (Fig. 5D). To strengthen our findings and determine if these effects could be seen at the transcriptional level, we separately isolated the epithelial and immune cells from the tumors and assessed RNA expression of known downstream products for each pathway. We found that the NLRP3 inflammasome product pro-*IL1B* was correlated not only to *Nlrp3* expression but also to *Sting* expression in the CRC cells (Fig. 5E). Similarly, expression of the STING pathway

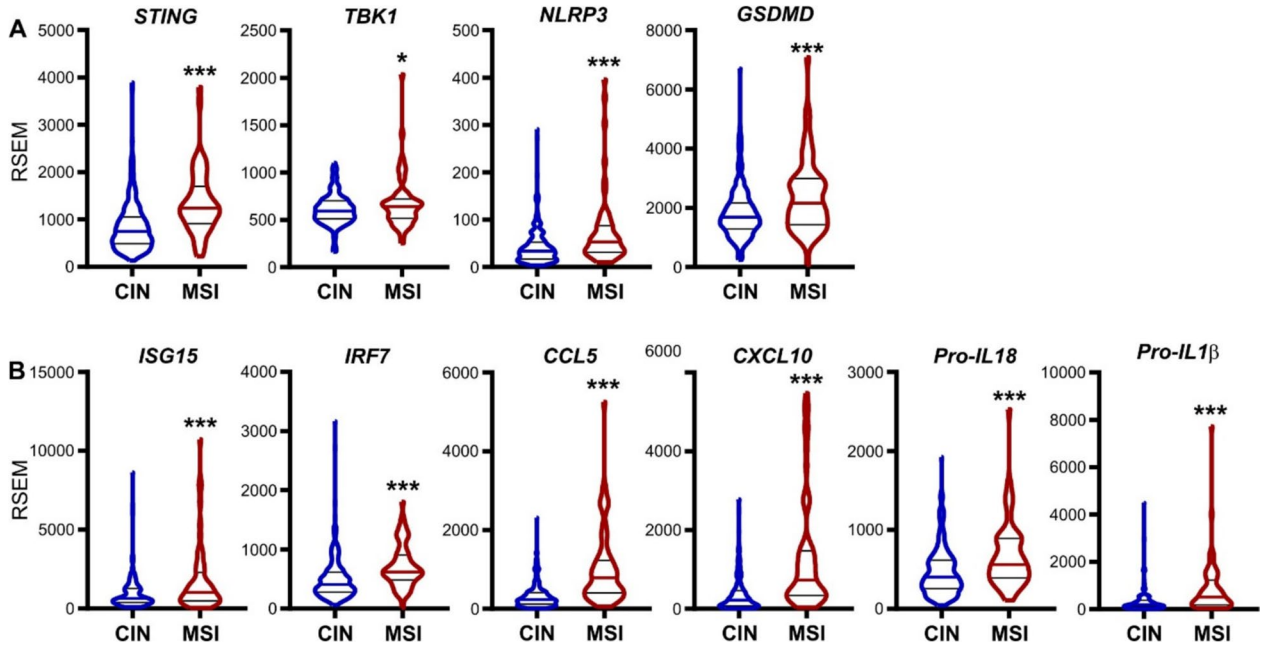

Fig. 4 Expression of NLRP3 and cGAS/STING pathways correlate with each other. **A** RNA sequencing for the expression of cGAS/STING and NLRP3 signaling pathway mediators in human CIN and MSI colorectal cancers from the PanCancer Atlas CRC dataset on the TCGA database. Y-axis units are RNA-Seq by Expectation–Maximization (RSEM). **B** Expression of major products of the cGAS/STING and NLRP3 inflammasome signaling pathways. The * symbols show significance of the indicated bar relative to CIN: $*p = 0.05$, $***p < 0.001$ (t-test)

product *Ccl5* was correlated not only to CRC *Sting* expression but also to *Nlrp3* expression. Given that we have shown CCL5 to be critical for recruitment of CD8+ T cells into the tumor microenvironment, we examined the immune cell component from the harvested tumors and looked at the relationship of *Sting* and *Nlrp3* expression to *Cd8a* expression in the immune population [6]. This showed that both *Sting* and *Nlrp3* expression in the CRC cells are correlated with *Cd8a* expression in the immune compartment of tumors but that neither *Sting* nor *Nlrp3* expression in the immune cells themselves correlated with *Cd8a* expression in these same cells (**Fig. S4**). These data indicate that these two PRRs each contribute to promoting CD8+ T cell-mediated antitumor immunity specifically in CRC cells and that they may work together to accomplish this.

Given the unique immune context of the intestine, which contains abundant PRR ligands due to its proximity to the intestinal flora, we next moved to an orthotopic model where the MSI and CIN MC38 CRC cells are endoscopically injected into the colonic wall of immunocompetent mice [2, 6]. MSI CRCs in this model had a higher percentage of NLRP3 and STING expressing tumor cells, suggesting that MSI CRCs are more sensitive to microbial signals that activate these pathways (Fig. 6A). Regardless of tumor type, expression of pSTING and NLRP3 in the CRC cells was highly correlated (Fig. 6B). To better elucidate the causal importance of NLRP3 to enhanced antitumor immunity, we treated orthotopically implanted mice repeatedly with the NLRP3 inhibitor MCC950 (Fig. 6C) [18]. This significantly decreased the activation of CD8+ T cells in MSI CRCs and the draining mesenteric lymph nodes (MLNs) (Figs. S5, S6). In addition, we confirmed the importance of STING by showing that orthotopically implanted $MSI^{StingKD}$ CRC cells expressed lower amounts of NLRP3 and recruited fewer activated CD8+ T cells than did the control tumors (Fig. 6D). This is consistent with our in vitro observations of CD8+ T cell activation (Fig. 3). We further confirmed the importance of STING to the efficacy of ICI treatment by showing that the STING agonist ADU-S100 increases antitumor immunity in the TME and draining mesenteric lymph nodes in mice treated with anti-PD1 (Fig. S6). Collectively, these results indicate that activation of the NLRP3 inflammasome may be an important contributor to cGAS/STING-mediated antitumor immunity in CRC, may contribute to TIL activation in MSI CRCs, and be an important therapeutic target for CIN CRCs.

NLRP3 activates cGAS/STING-mediated antitumor immunity in primary mouse and human CRCs

Although cell lines are extremely valuable tools, we sought to confirm that the enhancement of cGAS/STING by NLRP3 activation was not an artifact of the MC38 CRC cell line but a bona fide biological mechanism. To do this, we established

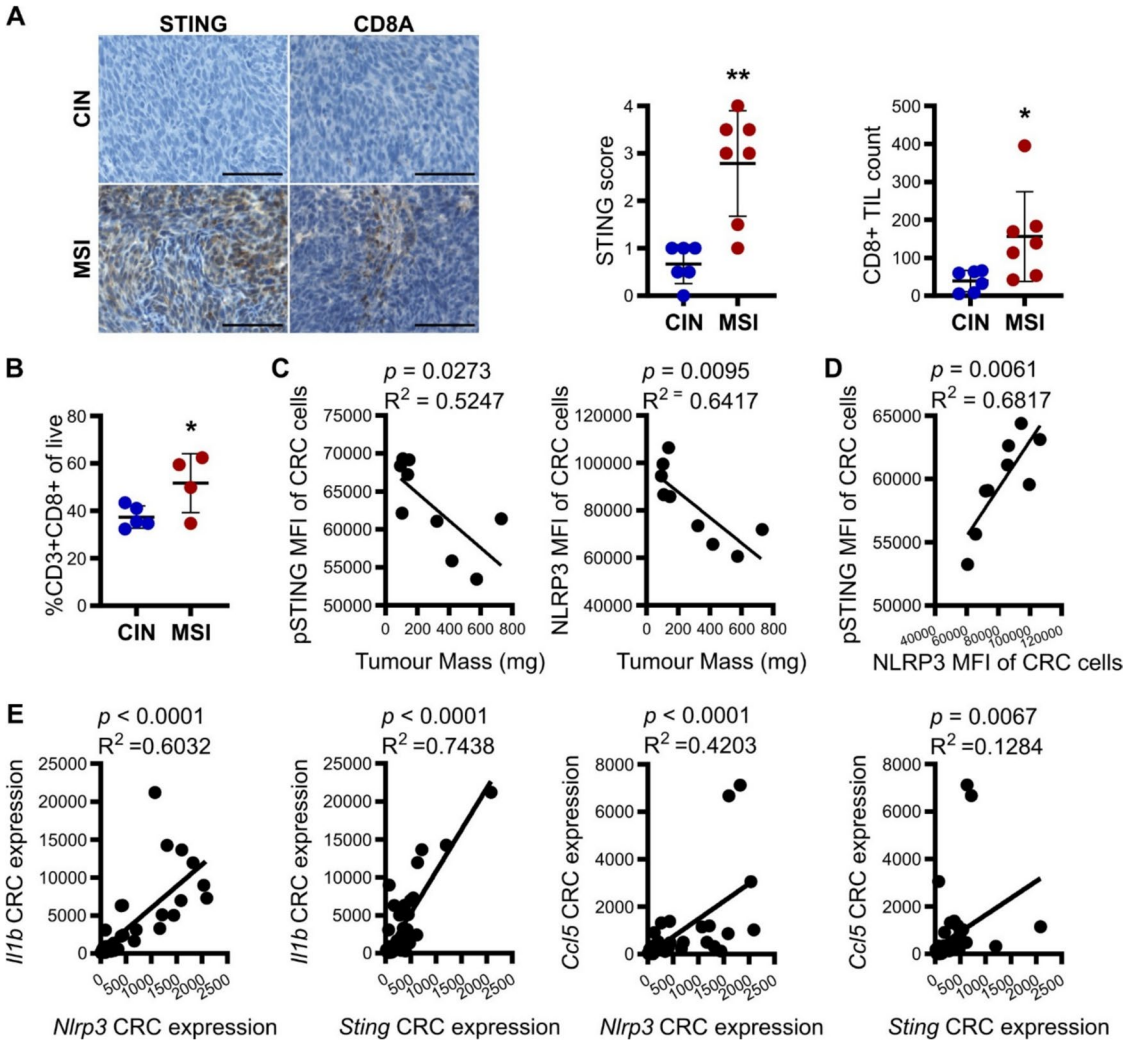

Fig. 5 NLRP3 and cGAS/STING are coregulated in CRC cells in vivo. MSI and CIN MC38 CRC cells were subcutaneously implanted in immunocompetent mice. **A** Expression of STING in CRC cells and infiltration by CD8+ T cells was evaluated by IHC. Scale bar = 100 µm. **B** CD8+ T cell infiltration into tumors was quantified by flow cytometry. **C, D** pSTING and NLRP3 expression in the CRC cells was quantified in isolated CRC cells by flow cytometry and then correlated with tumor size (**C**) or with each other (**D**). **E** Correlation between the expression of indicated genes in CRC cells isolated from subcutaneous tumors. CRC cells were isolated and qPCR was performed on RNA extracted from the purified tumor cells. For panels A-B, the * symbols show significance of MSI compared to CIN: $*p<0.05$, $**p<0.01$ (t-test). Panels C, D, E: Linear regression (C.I. = 95%) with the Pearson correlation R^2 and *p*-values reported on each graph

primary organoids from CRCs induced in wild type mice repeatedly administered azoxymethane (AOM) to induce CRC [6, 24]. We created an MSI variant of these organoids (Mlh^{KD}) by stably knocking down *Mlh1*. As seen with the MC38 CRC cells, dual stimulation increased expression of *Ccl5* and *Cxcl10* more than either agonist alone, especially for the $Mlh1^{KD}$ cells (Fig. 7A). In addition, we observed stronger activation of OT-I CD8+ T cells by the $Mlh1^{KD}$ organoids than the control CIN-like Ctl organoids (Fig. 7B), a difference that was enhanced by activation of either NLRP3 or cGAS/STING alone and most strongly enhanced by dual stimulation of both pathways (Fig. 7C).

To further extend the significance of NLRP3 and cGAS/STING cooperativity, we generated primary organoids from human CRCs and, for each patient's samples, created an MSI variant by knocking-down *MLH1* expression ($MLH1^{KD}$). Stimulation of either cGAS/STING or NLRP3 upregulated expression of IFN-associated chemokines *CCL5*, *CXCL10* and *ISG15* (Fig. 7D). Expression of each of these was even further enhanced by dual stimulation of cGAS/STING and NLRP3 in both the MSI and CIN organoid variants from each patient (Fig. 7D). These findings confirm that dual stimulation of NLRP3 and cGAS/STING pathways is an attractive therapeutic strategy for increasing the ability of

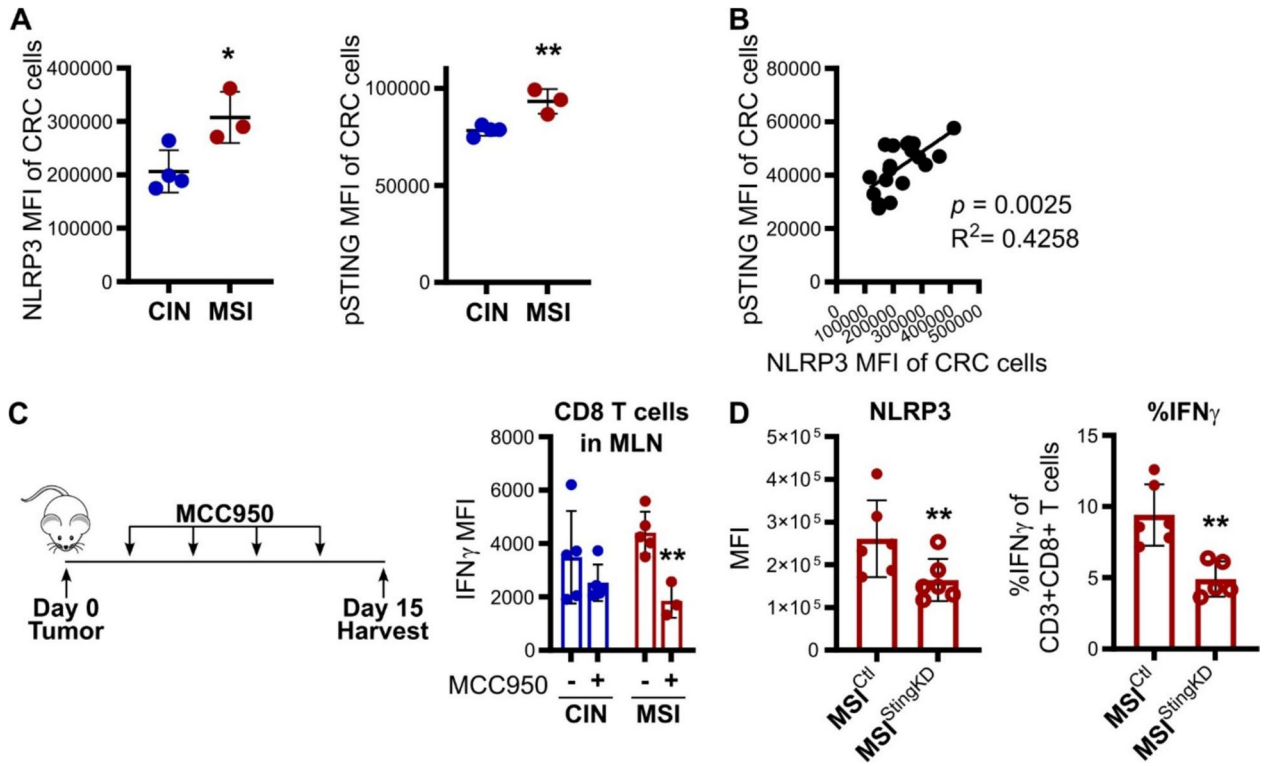

Fig. 6 NLRP3 and cGAS/STING in CRC cells jointly promote antitumor immunity in vivo. MSI and CIN CRC cells were orthotopically implanted into the colons of immunocompetent mice via non-invasive colonoscopy. pSTING and NLRP3 expression in the isolated CRC cells were quantified by flow cytometry (**A**) and analyzed for correlation (**B**). **C** Mice implanted with orthotopic MSI and CIN CRC cells were treated every 3 days with 20 mg/kg MCC950 via IP injection before harvesting tumors, MLNs and spleen for flow analysis. **D** $MSI^{StingKD}$ or control cells were orthotopically implanted in the colons of immunocompetent mice and then tumors were harvested and evaluated by flow for NLRP3 expression in the tumor cells or infiltration by activated CD8+ T cells. All panels show representative data from N ≥ 3 experiments. For panels A, C, D, the * symbols show significance of MSI compared to CIN: $*p < 0.05$, $**p < 0.01$ (t-test). Panels B: Linear regression (C.I. = 95%) with the Pearson correlation R^2 and *p*-values reported on each graph

CIN CRC cells to activate CD8+ T cell-mediated antitumor immunity (Fig. 8).

Discussion

Most CRCs are poor stimulators of antitumor immunity and are resistant to currently available immunotherapies. We show here that NLRP3 activation specifically in CRC cells enhances cGAS/STING signaling, thereby setting up a positive feedback loop that boosts production of IFN-stimulated genes, secretion of the T cell recruiting chemokines CCL5 and CXCL10, and activation of CD8+ T cells following their infiltration into the tumors. While we show that dual activation of these pathways is strongest in the immunogenic MSI CRC subtype, dual treatment with agonists of both NLRP3 and cGAS/STING also significantly increased CD8+ T cell activation in CIN CRCs. Our findings indicate that stimulating NLRP3 and cGAS/STING directly in CRC cells themselves is a promising therapeutic strategy for enhancing antitumor immunity even in typically cold tumors.

Inflammation is very much a dual-edge sword in cancer [36]. While high grade and chronic inflammation both predispose to cancer and accelerate its progression, low level acute inflammation can potentiate the activation of tumor-targeting cytotoxic T cells by providing necessary costimulatory signals [36]. Although formation of the NLRP3 inflammasome is typically associated with chronic inflammation, our findings illustrate that it can also enhance dsd CD8+ T cell activation by feeding into the cGAS/STING pathway and increasing production of IFN-stimulated genes [14–17]. This specifically occurred when stimulation was limited to the CRC cells themselves, indicating that intracellular context is a critical determinant of the outcome of PRR activation in the TME. This provides important insight into how crosstalk between innate signaling pathways in specific cell types can fine tune the overall tumor immune microenvironment and may also shed light on the differential consequences of IFN pathway activation in cancer. While abundant evidence supports the importance of type I IFN

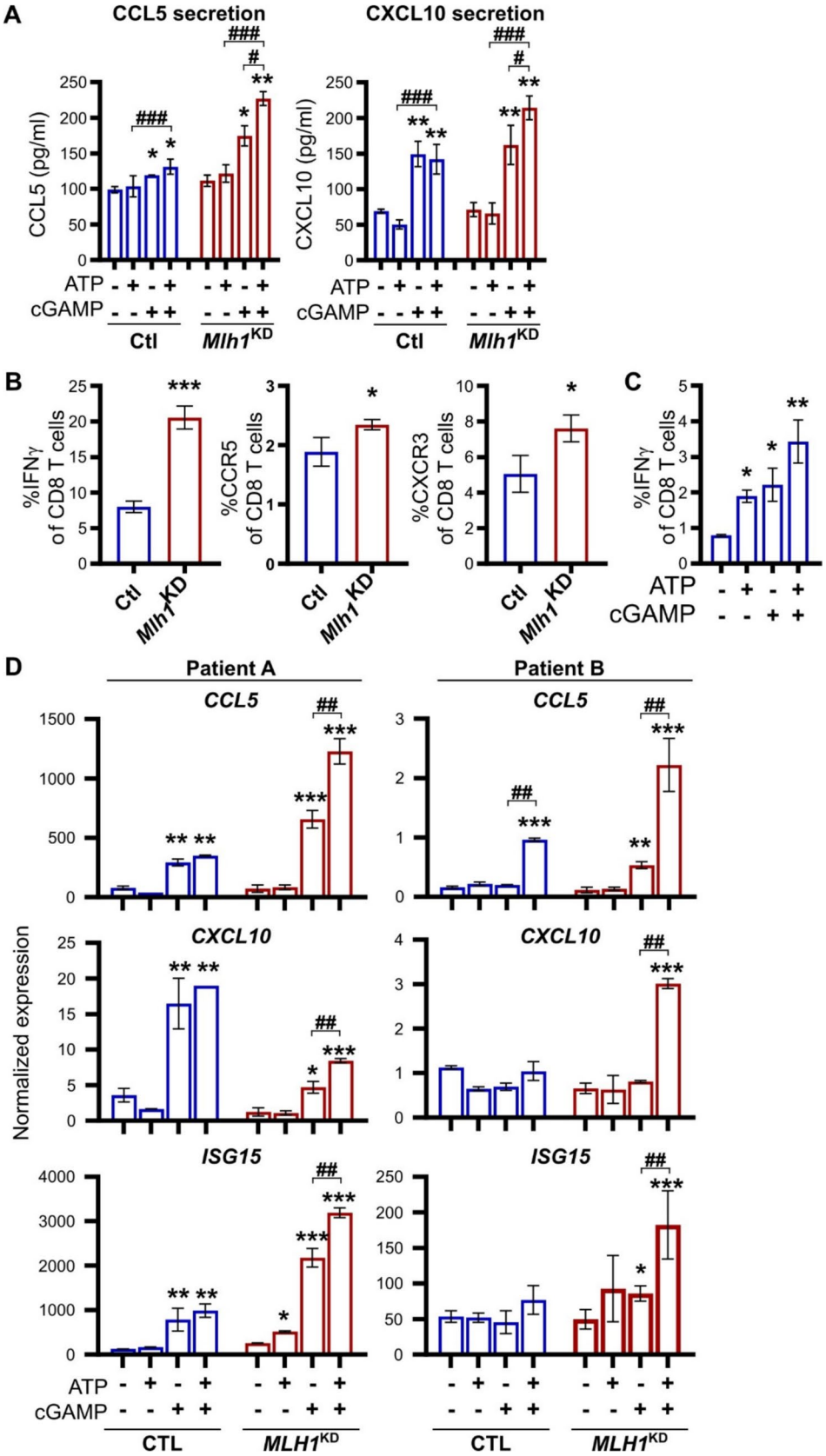

Fig. 7 NLRP3 and cGAS/STING cooperatively regulate antitumor immunity in primary mouse and human CRC cells. **A–C** Primary organoids were generated from CRC tumors induced in mice by repeated injection of AOM. *Mlh1* was then stably knocked down to create an MSI variant ($Mlh1^{KD}$). **A** Organoids were stimulated for 24 h with 9 µg/ml 2'-3'-cGAMP and/or 2 mM ATP before their supernatant was harvested and secreted cytokines were assessed by flow cytometric bead array. **B, C** Organoids were treated as in A and then washed before pulsing with SIINFEKL and coculturing with OT-I CD8+ T cells for 48 h. T cell activation was assessed by flow cytometry. (B) shows $Mlh1^{KD}$ cells while (C) shows both $Mlh1^{KD}$ and Ctl cells. **D** Primary organoids were generated from the resected tumors of two different CRC patients. *MLH1* was then stably knocked down in each to create an MSI variant ($MLH1^{KD}$). Organoids were stimulated for 24 h with 9 µg/ml 2'-3'-cGAMP and/or 2 mM ATP. RNA was then collected and gene expression was evaluated by qPCR. All panels show representative data from $N \geq 3$ experiments each with 2–4 biological replicates per experiment. For all panels, the * symbols show significance of the indicated bar relative to the corresponding vehicle control: $^{*}p \leq 0.05$, $^{**}p \leq 0.01$, $^{***}p \leq 0.001$ (t-test). For all panels, the # symbols show significance between the two indicated samples: $^{\#}p \leq 0.05$, $^{\#\#}p \leq 0.01$, $^{\#\#\#}p \leq 0.001$ (ANOVA)

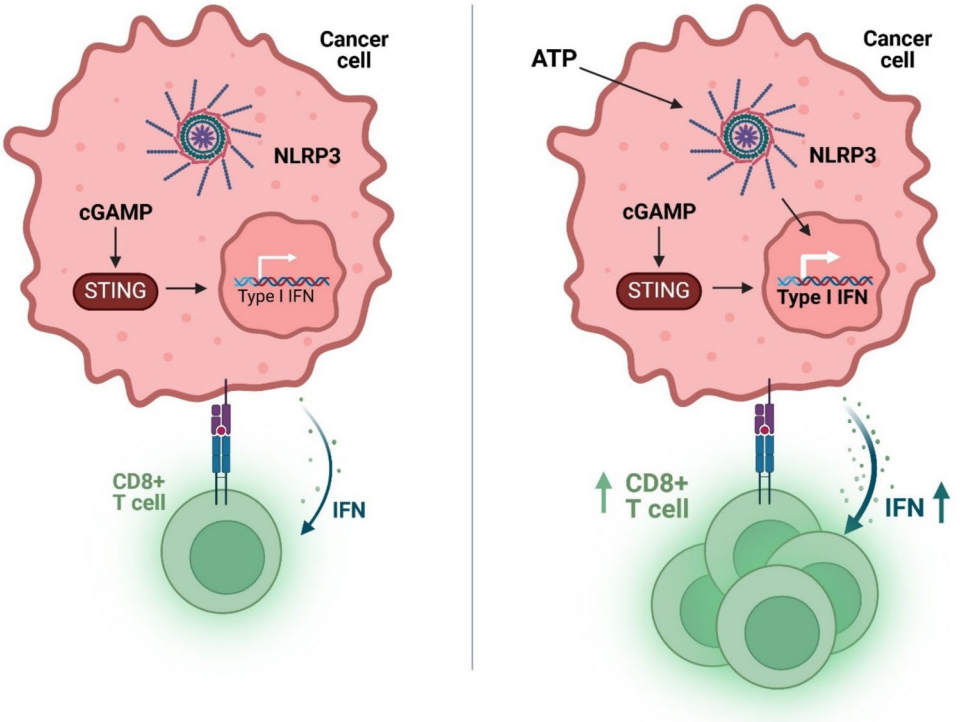

Fig. 8 Working model. Dual stimulation of NLRP3 and cGAS/STING specifically within cancer cells results in higher activation of CD8+ T cells than activation of either pathway alone

in promoting CD8+ T cell-mediated antitumor immunity, the tumor promoting effects of these IFNs is being increasingly recognized [37]. What ultimately determines whether cGAS/STING activation is beneficial or harmful in a given tumor thus likely depends on both the cell composition of the TME as well as what other PRRs are being activated within each cell. This is consistent with growing information about differences in the biology of individual cell types and their contribution to inflammation [38]. It is thus essential to better understand the interplay between different PRR pathways such as NLRP3 and cGAS/STING since doing so may uncover important opportunities for selectively modulating the pathways in a specific cell type to alter the balance between tumor-promoting inflammation and tumor-protective T cell responses in a given tumor. For example, given the ability of NLRP3 in immune cells to promote inflammation that could promote tumor growth or lead to tissue destruction over the prolonged course of therapy, our data suggests that targeted delivery of an NLRP3 agonist to the tumor cells themselves would be the safest approach to benefitting from its ability to activate CD8+ T cell-mediated antitumor immunity. Indeed, some benefit for such a strategy has recently been reported where intratumoral delivery of an NLRP3 agonist in conjunction with systemic checkpoint inhibitors promoted some measures of antitumor immunity with only mild associated toxicities [39]. Our finding suggest that improved delivery methods for such an agonist directly into the tumor cells could help mitigate the toxicities while improving the antitumor immune response.

The ability of cGAS/STING signaling to activate the NLRP3 inflammasome is well documented and seems to involve both transcriptional upregulation of NLRP3 pathway mediators as well as the induction of potassium efflux that triggers inflammasome assembly [12, 13]. This is consistent with our findings of correlation between cGAS/STING activation and NLRP3 expression in the CRC cells in addition to the increase in ASC specks we identified upon dual stimulation. In contrast, the mechanism by which NLRP3 enhances cGAS/STING signaling is not yet clear and contradicts several previous studies that found NLRP3 activation to repress cGAS/STING signaling [40, 41]. One possible reason for this discrepancy is the cell type in which NLRP3 was examined since most of the previous reports looked at NLRP3 activation in myeloid cells. Additionally, it is possible that activation of the NLRP3 inflammasome could lead to caspase-1-mediated DNA damage, including mitochondrial DNA oxidation, that results in release of the damaged DNA into the cytosol where cGAS can detect it [13]. However, our data indicate that the caspase-1 inflammasome is not required for amplification of cGAS/STING signaling by NLRP3 and that it instead proceeds via an inflammasome-independent function of NLRP3 [42]. While more conclusive evidence for this requires development of highly specific inhibitors of caspase-11 and ASC, caspase-1-independent NLRP3 pathways have previously been described that could underlie its activation of cGAS/STING. In one such non-canonical pathway, NLRP3 activation generates reactive oxygen species (ROS) in the mitochondria that lead

to mitophagy and production of damaged DNA that could activate cGAS [43]. Involvement of such a mechanism is supported by our findings of enhanced ROS production by dual stimulation with ATP and cGAMP. NLRP3-mediated cGAS/STING activation could also result from its role as a stress sensor, especially in MSI CRCs that experience high levels of genotoxic or ER stress induced by excessive point mutations and aberrant proteins [44]. Alternatively, NLRP3 could be activated by signaling from the high levels of immune cells that infiltrate MSI CRCs or by specific microbial taxa that have been found to be enriched in MSI CRCs [5, 45]. Which of these pathways is activated by a particular stimulus likely depends on both cell type-dependent effects as well as the context in which the signal is received. This is exemplified by our consistent observation that NLRP3 induces greater activation of cGAS/STING in MSI compared to CIN CRC cells where the former have much higher baseline activation of the cGAS/STING pathway [5, 6].

Further research is needed to uncover the detailed mechanism by which innate immune sensors such NLRP3 can contribute to regulation of productive antitumor immunity while minimizing their contribution to tumor-promoting inflammation. The importance of doing so is highlighted by our current work showing how NLRP3 stimulation in CRC cells can directly boost the ability of cGAS/STING to drive CD8+ T cell-mediated antitumor immunity even in CIN CRC tumors that are normally immunologically cold. Developing therapies that exploit the crosstalk between these pathways is thus a promising strategy to maximize immunotherapy response rates in all CRCs while minimizing the induction of inflammation that promotes tumor growth and leads to adverse therapeutic events.

Supplementary Information The online version contains supplementary material available at https://doi.org/10.1007/s00262-025-04088-y.

Acknowledgements The authors thank Rose-Marie Cornand, Dan McGinn, Cheryl Santos, Daming Li, Dr. Xuejun Sun, Dr. Anne Galloway and Dr. Lei Li as well as the Faculty of Medicine and Dentistry ACE and Imaging Cores at the University of Alberta for technical support.

Author contributions C.M. conceived of the project, designed and performed experiments, analyzed data and wrote the manuscript. D. S. provided human CRC tissue samples and edited the manuscript. K. B. conceived of the project, analyzed data, wrote the manuscript and secured funding.

Funding This project was supported by funding from the Canadian Institutes of Health Research (grant 407882), the Natural Sciences and Engineering Research Council of Canada (grant RGPIN-2016–05152), the Canadian Foundation for Innovation (grant 37832), and the University Hospital Foundation (KB).

Data availability The data that support the findings of this study are not openly available due to reasons of sensitivity and are available from the corresponding author upon reasonable request. Data are located in controlled access data storage at the University of Alberta.

Declarations

Conflict of interests The authors declare no competing interests.

Ethics approval All animal work was approved by the Cross Cancer Institute's Animal Care Committee (AC19248, AC23259). All work with human samples was approved by the Health Research Ethics Board of Alberta Cancer Committee and performed after obtaining informed patient consent (HREBA.CC-15–0112).

References

1. Mowat AM, Agace WW (2014) Regional specialization within the intestinal immune system. Nat Rev Immunol 14:667–685. https://doi.org/10.1038/nri3738
2. Cerovic V, Pabst O, Mowat AM (2025) The renaissance of oral tolerance: merging tradition and new insights. Nat Rev Immunol 25:42–56. https://doi.org/10.1038/s41577-024-01077-7
3. Kloor M, von Knebel DM (2016) The immune biology of microsatellite-unstable cancer. Trends Cancer 2:121–133. https://doi.org/10.1016/j.trecan.2016.02.004
4. Bakhoum SF, Cantley LC (2018) The multifaceted role of chromosomal instability in cancer and its microenvironment. Cell 174:1347–1360. https://doi.org/10.1016/j.cell.2018.08.027
5. Mowat C, Dhatt J, Bhatti I, Hamie A, Baker K (2023) Short chain fatty acids prime colorectal cancer cells to activate antitumor immunity. Front Immunol 14:1190810. https://doi.org/10.3389/fimmu.2023.1190810
6. Mowat C, Mosley SR, Namdar A, Schiller D, Baker K (2021) Anti-tumor immunity in mismatch repair-deficient colorectal cancers requires type I IFN-driven CCL5 and CXCL10. J Exp Med. https://doi.org/10.1084/jem.20210108
7. Lu C, Guan J, Lu S et al (2020) DNA sensing in mismatch repair-deficient Tumor cells is essential for anti-Tumor immunity. Cancer Cell. https://doi.org/10.1016/j.ccell.2020.11.006
8. Samson N, Ablasser A (2022) The cGAS-STING pathway and cancer. Nat Cancer 3:1452–1463. https://doi.org/10.1038/s43018-022-00468-w
9. Yu R, Zhu B, Chen D (2022) Type I interferon-mediated tumor immunity and its role in immunotherapy. Cell Mol Life Sci 79:191. https://doi.org/10.1007/s00018-022-04219-z
10. Iurescia S, Fioretti D, Rinaldi M (2018) Targeting cytosolic nucleic acid-sensing pathways for cancer immunotherapies. Front Immunol 9:711. https://doi.org/10.3389/fimmu.2018.00711
11. Zhivaki D, Kagan JC (2021) NLRP3 inflammasomes that induce antitumor immunity. Trends Immunol 42:575–589. https://doi.org/10.1016/j.it.2021.05.001

12. Liu J, Zhou J, Luan Y, Li X, Meng X, Liao W, Tang J, Wang Z (2024) cGAS-STING, inflammasomes and pyroptosis: an overview of crosstalk mechanism of activation and regulation. Cell Commun Signal 22:22. https://doi.org/10.1186/s12964-023-01466-w
13. Swanson KV, Junkins RD, Kurkjian CJ et al (2017) A noncanonical function of cGAMP in inflammasome priming and activation. J Exp Med 214:3611–3626. https://doi.org/10.1084/jem.20171749
14. Vafaei S, Taheri H, Hajimomeni Y, Fakhre Yaseri A, Abolhasani Zadeh F (2022) The role of NLRP3 inflammasome in colorectal cancer: potential therapeutic target. Clin Transl Oncol 24:1881–1889. https://doi.org/10.1007/s12094-022-02861-4
15. Perera AP, Sajnani K, Dickinson J, Eri R, Körner H (2018) NLRP3 inflammasome in colitis and colitis-associated colorectal cancer. Mamm Genome 29:817–830. https://doi.org/10.1007/s00335-018-9783-2
16. Ghiringhelli F, Apetoh L, Tesniere A et al (2009) Activation of the NLRP3 inflammasome in dendritic cells induces IL-1beta-dependent adaptive immunity against tumors. Nat Med 15:1170–1178. https://doi.org/10.1038/nm.2028
17. Theivanthiran B, Evans KS, DeVito NC et al (2020) A tumor-intrinsic PD-L1/NLRP3 inflammasome signaling pathway drives resistance to anti-PD-1 immunotherapy. J Clin Invest 130:2570–2586. https://doi.org/10.1172/JCI133055
18. Shi F, Wei B, Lan T, Xiao Y, Quan X, Chen J, Zhao C, Gao J (2021) Low NLRP3 expression predicts a better prognosis of colorectal cancer. Biosci Rep. https://doi.org/10.1042/BSR20210280
19. Cornista AM, Giolito MV, Baker K et al (2023) Colorectal cancer immunotherapy: state of the art and future directions. Gastro Hep Adv 2:1103–1119. https://doi.org/10.1016/j.gastha.2023.09.007
20. Ran FA, Hsu PD, Wright J, Agarwala V, Scott DA, Zhang F (2013) Genome engineering using the CRISPR-Cas9 system. Nat Protoc 8:2281–2308. https://doi.org/10.1038/nprot.2013.143
21. Moffat J, Grueneberg DA, Yang X et al (2006) A lentiviral RNAi library for human and mouse genes applied to an arrayed viral high-content screen. Cell 124:1283–1298. https://doi.org/10.1016/j.cell.2006.01.040
22. Yang J, Sanderson NS, Wawrowsky K, Puntel M, Castro MG, Lowenstein PR (2010) Kupfer-type immunological synapse characteristics do not predict anti-brain tumor cytolytic T-cell function in vivo. Proc Natl Acad Sci U S A 107:4716–4721. https://doi.org/10.1073/pnas.0911587107
23. Schneider CA, Rasband WS, Eliceiri KW (2012) NIH image to ImageJ: 25 years of image analysis. Nat Methods 9:671–675. https://doi.org/10.1038/nmeth.2089
24. Baker K, Rath T, Flak MB et al (2013) Neonatal Fc receptor expression in dendritic cells mediates protective immunity against colorectal cancer. Immunity 39:1095–1107. https://doi.org/10.1016/j.immuni.2013.11.003
25. Roper J, Tammela T, Akkad A, Almeqdadi M, Santos SB, Jacks T, Yilmaz OH (2018) Colonoscopy-based colorectal cancer modeling in mice with CRISPR-Cas9 genome editing and organoid transplantation. Nat Protoc 13:217–234. https://doi.org/10.1038/nprot.2017.136
26. Sato T, Stange DE, Ferrante M et al (2011) Long-term expansion of epithelial organoids from human colon, adenoma, adenocarcinoma, and Barrett's epithelium. Gastroenterology 141:1762–1772. https://doi.org/10.1053/j.gastro.2011.07.050
27. Miyoshi H, Stappenbeck TS (2013) In vitro expansion and genetic modification of gastrointestinal stem cells in spheroid culture. Nat Protoc 8:2471–2482. https://doi.org/10.1038/nprot.2013.153
28. Cancer Genome Atlas N (2012) Comprehensive molecular characterization of human colon and rectal cancer. Nature 487:330–337. https://doi.org/10.1038/nature11252
29. Hoadley KA, Yau C, Hinoue T et al (2018) Cell-of-origin patterns dominate the molecular classification of 10,000 Tumors from 33 types of cancer. Cell 173(291–304):e6. https://doi.org/10.1016/j.cell.2018.03.022
30. Sanchez-Vega F, Mina M, Armenia J et al (2018) Oncogenic signaling pathways in the cancer genome atlas. Cell 173(321–37):e10. https://doi.org/10.1016/j.cell.2018.03.035
31. Love MI, Huber W, Anders S (2014) Moderated estimation of fold change and dispersion for RNA-seq data with DESeq2. Genome Biol 15:550. https://doi.org/10.1186/s13059-014-0550-8
32. Mahlakoiv T, Hernandez P, Gronke K, Diefenbach A, Staeheli P (2015) Leukocyte-derived IFN-alpha/beta and epithelial IFN-lambda constitute a compartmentalized mucosal defense system that restricts enteric virus infections. PLoS Pathog 11:e1004782. https://doi.org/10.1371/journal.ppat.1004782
33. Weindel CG, Martinez EL, Zhao X et al (2022) Mitochondrial ROS promotes susceptibility to infection via gasdermin D-mediated necroptosis. Cell 185:3214–31.e23. https://doi.org/10.1016/j.cell.2022.06.038
34. Sharma BR, Karki R, Kanneganti TD (2019) Role of AIM2 inflammasome in inflammatory diseases, cancer and infection. Eur J Immunol 49:1998–2011. https://doi.org/10.1002/eji.201848070
35. Vijay-Kumar M, Gewirtz AT (2009) Flagellin: key target of mucosal innate immunity. Mucosal Immunol 2:197–205. https://doi.org/10.1038/mi.2009.9
36. Lichtenstern CR, Ngu RK, Shalapour S, Karin M (2020) Immunotherapy, Inflammation and colorectal cancer. Cells 9:E618. https://doi.org/10.3390/cells9030618
37. Cheon H, Wang Y, Wightman SM, Jackson MW, Stark GR (2023) How cancer cells make and respond to interferon-I. Trends Cancer 9:83–92. https://doi.org/10.1016/j.trecan.2022.09.003
38. Weavers H, Martin P (2020) The cell biology of inflammation: from common traits to remarkable immunological adaptations. J Cell Biol 219:e202004003. https://doi.org/10.1083/jcb.202004003
39. Nelson BE, O'Brien S, Sheth RA et al (2025) Phase I study of BMS-986299, an NLRP3 agonist, as monotherapy and in combination with nivolumab and ipilimumab in patients with advanced solid tumors. J Immunother Cancer 13:e010013. https://doi.org/10.1136/jitc-2024-010013
40. Ning L, Wei W, Wenyang J, Rui X, Qing G (2020) Cytosolic DNA-STING-NLRP3 axis is involved in murine acute lung injury induced by lipopolysaccharide. Clin Transl Med 10:e228. https://doi.org/10.1002/ctm2.228
41. Wu T, Gao J, Liu W, Cui J, Yang M, Guo W, Wang FY (2021) NLRP3 protects mice from radiation-induced colon and skin damage via attenuating cGAS-STING signaling. Toxicol Appl Pharmacol 418:115495. https://doi.org/10.1016/j.taap.2021.115495
42. Wang H, Wang Y, Du Q, Lu P, Fan H, Lu J, Hu R (2016) Inflammasome-independent NLRP3 is required for epithelial-mesenchymal transition in colon cancer cells. Exp Cell Res 342:184–192. https://doi.org/10.1016/j.yexcr.2016.03.009
43. Shimada K, Crother TR, Karlin J et al (2012) Oxidized mitochondrial DNA activates the NLRP3 inflammasome during apoptosis. Immunity 36:401–414. https://doi.org/10.1016/j.immuni.2012.01.009
44. Zheng W, Liu A, Xia N, Chen N, Meurens F, Zhu J (2023) How the Innate Immune DNA Sensing cGAS-STING Pathway Is Involved in Apoptosis. Int J Mol Sci. https://doi.org/10.3390/ijms24033029
45. Ugai T, Akimoto N, Haruki K et al (2023) Prognostic role of detailed colorectal location and tumor molecular features: analyses of 13,101 colorectal cancer patients including 2994 early-onset cases. J Gastroenterol 58:229–245. https://doi.org/10.1007/s00535-023-01955-2